Chinese Chemical Letters 35 (2024) 108491

Contents lists available at ScienceDirect

Chinese Chemical Letters

journal homepage: www.elsevier.com/locate/cclet

The guest CH_3CN molecule triggers solid-state photochromism in a Cu_2I_2-based MOF for advanced time-dependent encryption and inkless erasable printing

Meng-Juan Wang[a], Bo Li[b], Yong-Li Wei[a], Shu-Na Zhao[a,*], Shuang-Quan Zang[a,*]

[a] Henan Key Laboratory of Crystalline Molecular Functional Materials, Henan International Joint Laboratory of Tumor Theranostical Cluster Materials, Green Catalysis Center, and College of Chemistry, Zhengzhou University, Zhengzhou 450001, China
[b] College of Chemistry and Pharmaceutical Engineering, Nanyang Normal University, Nanyang 473061, China

ARTICLE INFO

Article history:
Received 20 February 2023
Revised 30 March 2023
Accepted 20 April 2023
Available online 28 April 2023

Keywords:
Stimuli-responsive materials
Spiropyran
Solid-state photochromism
Time-dependent encryption
Inkless erasable printing

ABSTRACT

It remains a big challenge to develop solid-state stimuli-responsive materials for time-dependent information encryption and inkless erasable printing with long retention times. Herein, a 2D Cu_2I_2-based MOF with photoresponsive spiropyran (SP) groups orderly installed on its skeleton is developed. The structural isomerization from SP to colored merocyanine (MC) form can be triggered by removing the CH_3CN guests. Besides, the degree of structural isomerization and the retention time can be adjusted by controlling the amount of CH_3CN guests, exhibiting dynamic photochromic behavior with multicolor states and tunable retention time. Based on these advantages, time-dependent information encryption is successfully achieved. Furthermore, the long retention time (>72 h) of the MC form under daylight conditions in the CH_3CN-removed Cu_2I_2-based MOF and good repeatability make it promising in various applications, such as temporary calendars, price-cards, billboards, and reusable identity cards. This work provides a novel design strategy to fabricate multi-functional MOF-based smart materials for challenging applications of time-dependent information encryption and inkless erasable printing.

© 2024 Published by Elsevier B.V. on behalf of Chinese Chemical Society and Institute of Materia Medica, Chinese Academy of Medical Sciences.

Stimuli-responsive smart materials have drawn considerable interest in the fields of data encryption, anticounterfeiting, smart window, erasable and inkless printing, and biological imaging agents owing to quick response towards external stimuli, such as heat, light, mechanical stress, pH, and voltage [1–11]. Currently, the most common smart materials have been concentrated on hydrogels, carbon materials, organic polymers, and crystalline liquids [12–16]. However, the responsive moieties in the material structures are usually disorder due to the low crystallinity of the above-mentioned smart materials. The disorder arrangement of responsive moieties inevitably makes it difficult to unveil the response mechanism and the structure-property relationships at the molecular level, thus limiting the development of new kinds of stimuli-responsive smart materials. Crystalline materials, particularly porous materials such as metal-organic frameworks (MOFs) with organic ligands arranged in a precise manner in a periodic lattice can provide a great chance to create novel stimuli-responsive materials due to the following features: (1) The responsive functional groups on the MOFs skeletons are uniformly installed and formed ordered arrays, which makes it much faster and more efficient to transfer the energy between external-stimulus signals and responsive sites [17–22]; (2) The high porosity of MOFs provides enough free volume for structure transformation of responsive groups, which is conducive to the reversible response in the solid state [23–26]; (3) The precise structures provide a great platform to investigate the response mechanism and structure-property relationships [27–29]. Owing to the above-mentioned advantages, many photochromic MOFs with stimuli-responsive groups such as azobenzene, diarylethene, and spiropyran have been reported to date and showed promising applications in the fields of adsorption and separation, optoelectronic devices, information storage and anticounterfeiting [26,30–34]. For example, the azobenzene photochromic moiety as the pendant group, guest molecules, or the organic linkers in the photochromic MOFs can modify the pore size and environment upon *cis/trans* switching of azobenzene groups, thus offering interesting applications in gas adsorption and separation [30–33]. Shustova and coworkers reported a series of photochromic MOFs by using spiropyran-based photochromic linkers, which showed dynamically controlled electronic behavior [26]. In another example, a photoresponsive 2D

* Corresponding authors.
E-mail addresses: zhaosn@zzu.edu.cn (S.-N. Zhao), zangsqzg@zzu.edu.cn (S.-Q. Zang).

https://doi.org/10.1016/j.cclet.2023.108491
1001-8417/© 2024 Published by Elsevier B.V. on behalf of Chinese Chemical Society and Institute of Materia Medica, Chinese Academy of Medical Sciences.

TSiMOF was prepared with hexamethyltrisilane groups orderly anchored on its surface [34]. The fluorescence of the TSiMOF can be turned on accompanied by an interesting surface transformation from superhydrophobic to hydrophilic after UV light irradiation due to the photochemical oxidation of superficial trimethylsilyl to hydroxyl groups. These make the TSiMOF very useful in fabricating various fluorescence patterns through directly etching on the Zn-TSiMOF film.

Notwithstanding the progress, most of the MOFs-based stimuli-responsive smart materials only showed one input signal (the external stimulus) and one output signal caused by the structure transformation of responsive groups with MOFs only as frameworks, limiting their applications in anticounterfeiting and information encryption. Integrating multiple external-stimuli and multiple and/or dynamic output signals in one system is crucial for a higher level of information encryption [35–37]. Particularly, time-dependent information encryption materials, which show multiple informational states on a time scale and only provided the correct information at a specific time, are more desired for higher security requirements [38–40]. Qu and coworkers recently generated 3D/4D codes based on a pyrene-based multicolor-fluorescence supramolecular system, which presented time-dependent dynamic fluorescent signals by tailoring the solvent composition [38]. Huang and coworkers developed another time-dependent information encryption using a pillar[5]arene-based host-guest invisible ink, in which the different information states were achieved by tailoring the fading rates [39]. The intrinsic properties of MOFs, such as tunable pore sizes, abundant guests, and facile functionalization can be very useful to initiate the structure transformation of responsive groups, control the degree of their structure transformation, and/or change their restoration time. However, it is still a great challenge to trigger the structure transformation of responsive groups on the MOFs' skeleton to develop time-dependent information encryption materials by modulating the intrinsic properties of MOFs.

In this work, we synthesized a 2D Cu_2I_2-based MOF (Cu_2I_2-TNDS·CH_3CN, TNDS = 1′,3′,3′-trimethyl-6-nitro-4′,7′-di(pyridin-4-yl)-spiro[*chromene*-2,2′-*indoline*]) with photoresponsive SP groups orderly installed on its skeleton. Then, the sample were treated under different temperatures, labeled as Cu_2I_2-TNDS·CH_3CN (without heating), Cu_2I_2-TNDS-100/Cu_2I_2-TNDS-150 (heating under 100 °C or 150 °C). The CH_3CN guests can block the structural isomerization of SP, thus, no color change happened under UV light irradiation for Cu_2I_2-TNDS·CH_3CN. When partly removing the CH_3CN guests at 100 °C, some SP groups in Cu_2I_2-TNDS-100 can be transformed into the colored MC form along with a color change from yellow to yellow-green in the solid state. When increasing the temperature to 150 °C, the CH_3CN guests were totally removed, Cu_2I_2-TNDS-150 presents blue-green color under UV light due to the higher structural isomerization of SP under the same external stimulus condition. Interestingly, the blue-green color of Cu_2I_2-TNDS-150 can fade to yellow-green at a specific time (10 min) under heating at 80 °C. By taking advantage of the multiple and dynamic informational states of the Cu_2I_2-TNDS system, time-dependent information encryption was successfully achieved. Furthermore, the long retention time (>72 h) of the MC form in Cu_2I_2-TNDS-150 under daylight conditions and better repeatability motivated us to use it as short-term reusable materials such as temporary calendars, price-cards, billboards and identity cards. This work provides a novel design strategy to fabricate multi-functional MOF-based smart materials for challenging applications of time-dependent information encryption and inkless erasable printing.

The as-obtained material, denoted here as Cu_2I_2-TNDS·CH_3CN, was characterized by single-crystal X-ray diffraction (SCXRD), thermal gravimetric analysis (TGA), FT-IR and elemental analysis. Cu_2I_2-TNDS·CH_3CN crystallizes in the monoclinic $I2/a$ space group. The asymmetric unit contains 1/2 Cu_2I_2 moiety, one TNDS pyridine bidentate ligands, and one CH_3CN molecule. As shown in Fig. 1a and Fig. S10 (Supporting information), each Cu(I) atom in the Cu_2I_2 cluster is tetrahedrally coordinated with two I atoms and two N atoms from different TNDS ligands. The Cu_2I_2 cluster further ligates by four TNDS ligands to form a 2D Cu_2I_2-TNDS layer with rhomboid pores (Fig. S11 in Supporting information). These 2D layers show an ABAB stacking order along the crystallographic a axis, and each layer is slightly shifted with respect to the next one (Fig. S12 in Supporting information). The guest CH_3CN molecules are located at the rhomboid pore and stabilized by hydrogen bonding interactions (Figs. S11 and S13 in Supporting information). Interestingly, the CH_3CN guests can be totally removed upon heating at 150 °C for 4 h accompanied by a single-crystal-to-single-crystal (SCSC) phase transition (Fig. S14 and Table S2 in Supporting information) [41], resulting in variations for unit cell parameters (a: −0.34%; b: +2.62% and c: −5.28%) and volume (−3.78%), even Cu_2I_2-TNDS-150 retains the original space group ($I2/a$) and 2D framework of Cu_2I_2-TNDS·CH_3CN. Although volume shrinkage appeared on Cu_2I_2-TNDS-150, it still provides enough free volume for the structure transformation of SP groups (Fig. 1a and Table S3 in Supporting information) [42].

A variable-temperature powder X-ray diffraction (PXRD) was carried out to further confirm the SCSC phase transition. As shown in Figs. 1b and c, the PXRD pattern of Cu_2I_2-TNDS·CH_3CN is not exactly the same as its simulated pattern, implying that even a small amount of the guest solvents loss can cause a slight distortion of the framework. As the temperature increases, the peaks at 7.033° in Cu_2I_2-TNDS·CH_3CN gradually disappear (Fig. S15 in Supporting information). While the peaks at 7.438° in Cu_2I_2-TNDS-150 start to appear at 100 °C. After heating at 150 °C for 20 min, an obvious structure transformation occurs with the appearance of a new peak at 12.042° and the disappearance of the peak at 11.253° in the PXRD pattern of Cu_2I_2-TNDS-150. TGA results show that the untreated and 100 °C-treated crystals display weight loss of 6.01% and 2.96% (calculated: 5.80%, 2.99%) due to the loss of two and one CH_3CN molecules, respectively. However, Cu_2I_2-TNDS-150 shows no weight loss up to 300 °C (Fig. 1d), revealing that the CH_3CN molecules have been lost completely. In addition, a typical C≡N vibration peak at 2245 cm^{-1} vanishes in the FT-IR spectrum of Cu_2I_2-TNDS-150, further confirming the loss of CH_3CN molecules (Fig. S16 in Supporting information). Furthermore, the PXRD result of the Cu_2I_2-TNDS-150 after treating with fresh CH_3CN solvent is well matched with Cu_2I_2-TNDS-150, indicating that the SCSC phase transition is irreversible after heating at 150 °C (Fig. S17 in Supporting information).

Surprisingly, Cu_2I_2-TNDS·CH_3CN and desolvated Cu_2I_2-TNDS-150 exhibit totally different photophysical properties upon photoirradiation. As shown in Fig. 1e, the Cu_2I_2-TNDS·CH_3CN crystals present yellow color under daylight, and their color keeps unchanged after irradiation with 365 nm UV light. Correspondingly, no new absorption band was appeared in the UV–vis spectra of Cu_2I_2-TNDS·CH_3CN after UV irradiation (Fig. S18a in Supporting information). While the Cu_2I_2-TNDS-100 and −150 show a color change from yellow to yellow-green and blue-green, respectively, under the same stimulus, as evidenced by appearing a new broad absorption band at about 590 nm in their UV–vis spectra (Figs. 1e and 2a, Fig. S18b in Supporting information). These phenomena indicate that the photochromism is occurred in the solid state of Cu_2I_2-TNDS-100 and −150, in which the SP photochromic unit in the TNDS ligands switches to the highly colored MC form (Fig. 2b). However, the intensity of the new absorption band is dependent on the temperature of the heating treatment (Fig. S18b). Thus, it can be speculated that the CH_3CN molecules in Cu_2I_2-TNDS·CH_3CN show a significant impact on the photoswitching be-

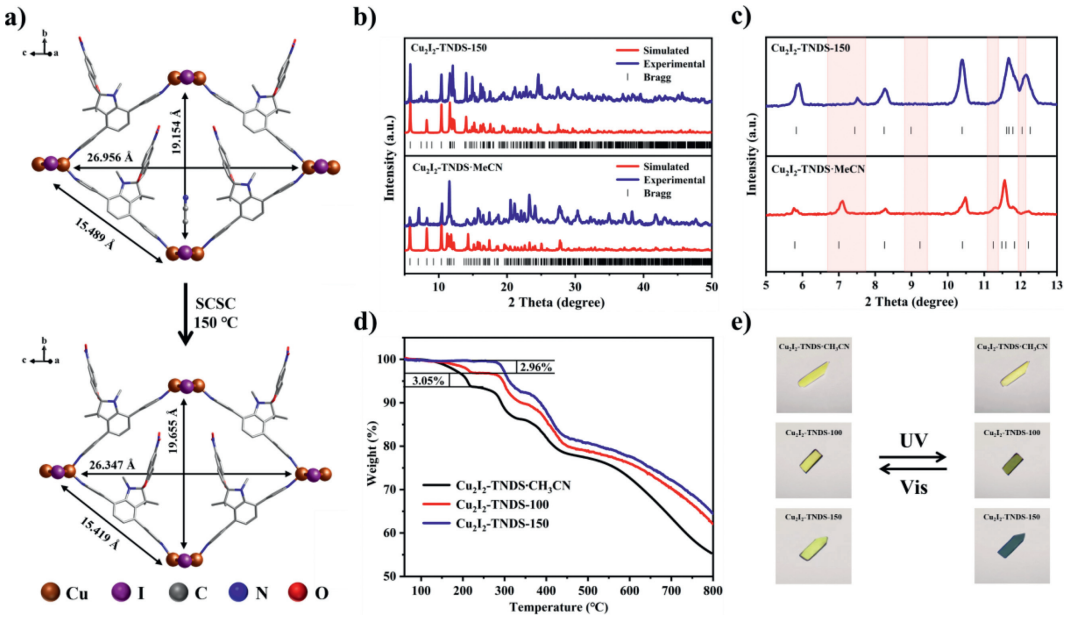

Fig. 1. (a) The SCSC phase transition progress of Cu_2I_2-TNDS•CH_3CN. (b, c) PXRD patterns of Cu_2I_2-TNDS•CH_3CN and Cu_2I_2-TNDS-150. (d) TGA curves for Cu_2I_2-TNDS•CH_3CN, −100, and −150. (e) Color changes of Cu_2I_2-TNDS•CH_3CN, −100 and −150 after UV irradiation.

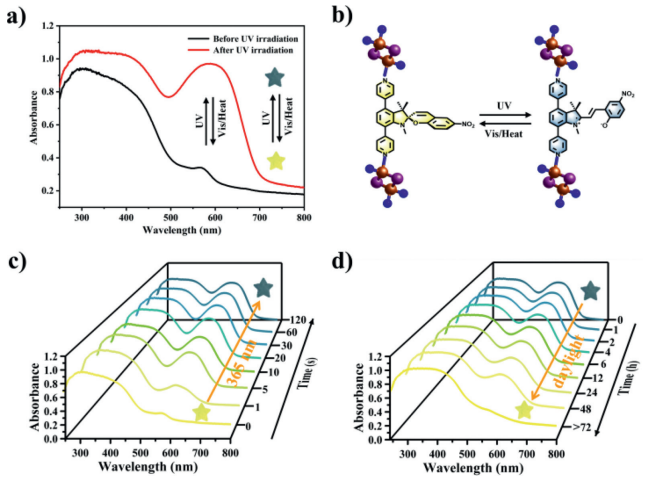

Fig. 2. (a) UV-vis absorption of Cu_2I_2-TNDS-150 powders before and after UV irradiation. (b) Reversible structural isomerization between SP and MC form in Cu_2I_2-TNDS-150 under different stimuli. Time-dependent UV–vis absorption spectra of Cu2I2-TNDS-150 powders (c) under 365 nm UV irradiation and (d) in daylight environment.

tween SP and MC. The formation of H-bonding interaction between the N atom in CH_3CN molecules and TNDS ligands from the adjacent layer would hinder the structural isomerization from SP to MC, whereas this interaction will be disappeared after removing CH_3CN molecules at 150 °C (Fig. S13). Theoretical calculations by using B3LYP-D3(BJ)/Def2-SV(P) method were further performed to investigate the effect of CH_3CN guests during the process of structural isomerization. The potential energy surfaces (PES) scan was used to investigate the SP isomerization of the simplified rhomboid Cu_2I_2-TNDS fragment of Cu_2I_2-TNDS·CH_3CN (Cu_2I_2-TNDS-150) by rotating the C=C double bond, namely the dihedral angle of C25 (C11) and C28 (C14) with respect to the C26 (C12)=C27 (C13) bond in the pyran ring, between SP (∼0°) and MC (∼180°) with the increment of 10° As shown in Fig. S19 and Table S4 (Supporting information), Cu_2I_2-TNDS·CH_3CN needs more energy (319.31 kcal/mol) to switch the SP form to the MC form in the solid state than Cu_2I_2-TNDS-150 (237.27 kcal/mol). The above results reveal that the CH_3CN guests limit the switch from SP to MC in Cu_2I_2-TNDS·CH_3CN.

The solid-state photochromic behavior of Cu_2I_2-TNDS-150 was investigated in details. With continuous UV-light irradiation, the absorption band at about 590 nm gradually increases, then reaches a photo-stationary state at a time point of 120 s (Fig. 2c). The new absorption band corresponds to the open-ring form with elongated π-conjugation, revealing that the UV light successfully triggers the switch from SP to MC in the solid state. After 72 h of uninterrupted testing in an ambient-light environment (Fig. 2d and Fig. S20 in Supporting information), there is not much difference appeared of the absorbance of the MC form in Cu_2I_2-TNDS-150 due to the strong restriction effect of the rigid structure of Cu_2I_2-TNDS-150, indicating the superior stability to most of the reported solid-state photochromic materials (Table S5 in Supporting information). In addition, the color of Cu_2I_2-TNDS-150 in the MC form could be restored to its initial state when heating at 80 °C for 30 min or irradiation under visible light for 60 min, demonstrating that the photochromism was well reversible under UV irradiations and heating/visible light treatment (Fig. S21 in Supporting information). This reversible process can be repeated at least 10 times (Fig. S22a in Supporting information). Furthermore, the PXRD patterns of Cu_2I_2-TNDS-150 collected before and after the 10 times photochromic cycle are exactly identical (Fig. S22b in Supporting information), proving the structural stability of Cu_2I_2-TNDS-150 under irradiation and heating treatment.

Based on the above results, multiple information states can be found in the Cu_2I_2-TNDS system. The yellow color of Cu_2I_2-TNDS·CH_3CN keeps unchanged under UV light irradiation, which can be denoted as state I. While the yellow-green and blue-green colors of Cu_2I_2-TNDS-100 and −150, which changes from yellow under the same external stimulus, can be denoted as state II and III, respectively. Interestingly, state III (blue-green color) can fade to state II (yellow-green color) at a specific time (10 min) under heating at 80 °C evidenced by their similar UV–vis absorption (Fig. S23 in Supporting information), whereas state II (yellow-green color) transforms to state I (yellow color) under the same stimulus. If heating at 80 °C for a longer time (such as 30 min), both state II (yellow-green color) and state III (blue-green color) restore to state

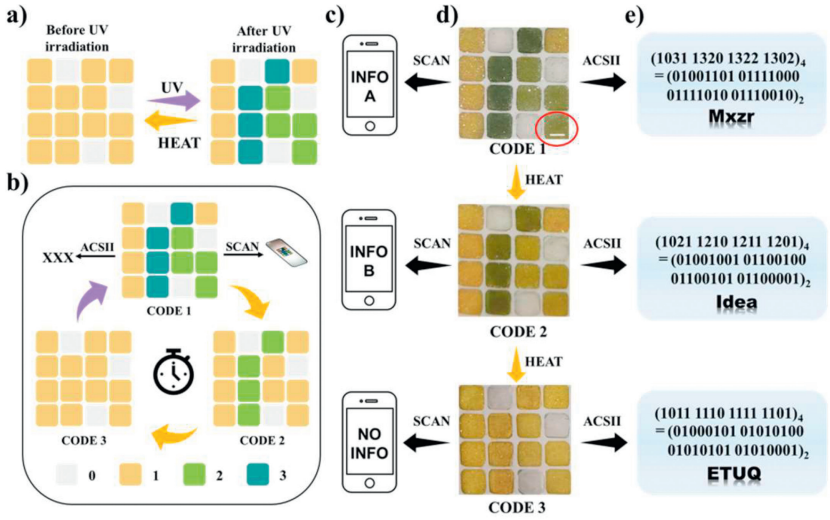

Fig. 3. (a) Schematic illustration of the 3D color code before and after UV irradiation. Yellow: Cu_2I_2-TNDS·CH_3CN; Yellow-green: Cu_2I_2-TNDS-100; Blue-green: Cu_2I_2-TNDS-150 in the 4 × 4 matrix after UV irradiation. (b) Schematic representations and (d) visible pictures of the 4 × 4 matrix on a time scale under the heating stimulus. White, yellow, yellow-green, and blue-green units represent the quaternary codes of "0", "1", "2", and "3", respectively (scale bar: 3 mm). (c) The corresponding information of 3D code was read using a smartphone. (e) Decoding of "Mxzr", "Idea" and "ETUQ" from the code at different heating times.

I (yellow color) (Fig. S24 in Supporting information). Such multiple information states and dynamic fading processes in the Cu_2I_2-TNDS system enable them to be potential candidates for time-dependent information encryption (Fig. S25 in Supporting information), which possesses higher security than traditional static technology.

3D color codes, which developed from the conventional black and white 2D code, can store additional information based on the colors [43]. It has drawn more and more attention due to the larger information storage capacity and a higher level of information security [44]. Thus, developing 3D color codes with dynamic color changes on the time scale is highly urgent. Based on the advantage of the multiple and dynamic informational states in the Cu_2I_2-TNDS system, a dynamic 3D code was designed from a conceptual point of view. As shown in Fig. 3a, this dynamic 3D code could be fabricated by specially arranging sample units to form a 4 × 4 matrix. In the initial state, all the sample units show similar yellow color, providing less information after scanning. When irradiated by UV light, the sample units with Cu_2I_2-TNDS·CH_3CN still keep the yellow color, whereas sample units with Cu_2I_2-TNDS-100 and −150 change to yellow-green and blue-green colors. Thus, the first-level information A (code 1) can be recognized. This information pattern code could dynamically transform on the time scale because the blue-green and yellow-green colors would revert back to yellow over time (Figs. 3b and d). Notably, the second-level information B (code 2) was accessible after heating at 80 °C for 10 min, at which point the blue-green color faded back to yellow-green and the yellow-green color faded back to yellow (Fig. 3c). Furthermore, this information disappeared with increasing heating time. Therefore, this dynamic 3D code underscores the importance of the right accesses (the external stimuli and a specific time). Otherwise, it would lead to no information or misinformation under wrong accesses (too long or too short heating time). Such a feature on the time scale offers a higher level of security.

To further investigate the applications of the Cu_2I_2-TNDS system in dynamic information encryption, another encryption and decryption approach was also performed. As displayed in Figs. 3b and d, the white container, Cu_2I_2-TNDS·CH_3CN, Cu_2I_2-TNDS-100, and −150 show different color changes under external stimuli, which represent the quaternary codes of "0", "1", "2", and "3", respectively. This Cu_2I_2-TNDS system is used to encode, store, and decode information "Idea" in a 4 × 4 matrix. Under daylight, the obtained quaternary codes can first convert to binary codes and then map to ASCII code to decrypt the blank information of "ETUQ" (Fig. 3e). The blank code would change to code 1 after UV irradiation, and the corresponding information "Mxzr" can be identified. The correct information of "Idea" stored in code 2 only can be read when treating code 1 at 80 °C for 10 min. If heating this 4 × 4 matrix for a longer time, code 2 would convert back to the blank code with the disappearance of the correct information. Thus, this 4 × 4 matrix produced three information codes as a function of heating time, namely, code 1, code 2, and code 3 (blank code), respectively. The correct information can only be read under specific conditions. Surprisingly, the security level of the encrypted information would be further enhanced by using more 4 × 4 matrices. For example, there are 9 combinations of information codes with only two 4 × 4 matrices (Fig. S26 in Supporting information). Only one of the 9 combinations, that is Code A_2 + Code B_1, can decode to the correct information "Read Book". Thus, the Cu_2I_2-TNDS system shows promising potential for constructing time-dependent information encryption with higher level security.

Furthermore, the superior stability of MC form in Cu_2I_2-TNDS-150 (>72 h in the ambient-light environment) inspired us to investigate its application in inkless erasable printing. The Cu_2I_2-TNDS-150-coated film (denoted as 150-coated film) was easily prepared by coating the well-grounded Cu_2I_2-TNDS-150 powder on an acrylate adhesive (ACA) (Fig. 4a). The Cu_2I_2-TNDS-150 powder is evenly distributed on ACA, confirming by the uniform dispersion of Cu, I, N, O and C atoms across the ACA matrix (Fig. S27 in Supporting information). The resulting 150-coated film retains the flexibility of ACA and its size can be adjusted according to the size of ACA (Fig. 4b).

By controlling the incidence of UV light through different stencils, printing contents were performed on the 150-coated film. Specifically, the 150-coated film was covered with a layer of the stencil and then exposed to 365 nm UV light (100% transparency) for more than 5 s to obtain the content with color (Fig. 4c). After the UV irradiation, the stencil was removed from the top of the 150-coated film to obtain a blue "Dragon Boat Racing" pattern printed on the yellowish background of the Cu_2I_2-TNDS-150 (Fig. 4d). The color contrast between the "Dragon Boat Racing" pattern and background was sufficient for visual reading of the content. These patterns can be preserved for more than 72 h under

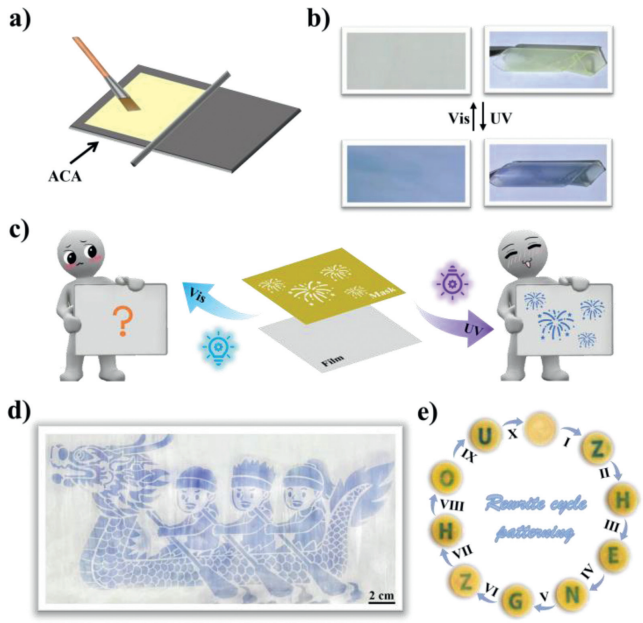

Fig. 4. (a) Schematic illustration of the process of the 150-coated film. (b) Before and after UV irradiation of the 150-coated film attached to a piece of paper or a flexible 150-coated film. (c) Diagram illustrations of the photomask printing processes. (d) The patterning application of the 150-coated film. (e) The records of the writing and erasing processes. (I) UV irradiation on Mask 1; (II-IX) Erasure by heating, then UV irradiation on different Masks 2–9; (X) Erasure by heating.

daylight conditions, which is enough for temporary uses (Fig. S28 in Supporting information). Whereas, a quick erase of the printed content was achieved by irradiating it under visible light for 4 h. Repeated printing of different contents on the same film showed no notable loss in the contrast, illustrating good repeatability of the 150-coated film (Fig. S29 in Supporting information). Given the exciting and reversible solid-state photochromic performance, the applications in rewritable patterns and short-term reusable displays were further realized based on the Cu_2I_2-TNDS-150 material. As illustrated in Fig. 4e, "Z H E N G Z H O U" letters would be appeared and disappeared in order in the writing-erasure cycles by using corresponding stencils. Even the last letter "U" is clear enough for reading, suggesting the excellent fatigue resistance of the Cu_2I_2-TNDS-150 material.

Moreover, the Cu_2I_2-TNDS-150 material can be used for the production of short-term reusable-display products, such as temporary calendars (Fig. 5a) and short-term price-card for supermarkets (Fig. 5b), which significantly benefits to waste paper reduction and forest conservation. The 150-coated film with adjustable size can also be used for fabricating the large-size reusable "billboards" (Fig. 5c), which can serve as an eco-friendly information display by reducing white pollution from a large number of single-use billboards. Owing to the advantage of information self-destruction without a trace by the heating treatment, the 150-coated film was fabricated for short-term identity cards (Fig. 5d). Thus, it not only can protect personal information but also can be reused.

In summary, a Cu_2I_2-TNDS system was successfully designed and synthesized, which exhibits dynamic photochromic behaviors with multicolor states and tunable retention time. The structural isomerization from SP to colored MC form in Cu_2I_2-TNDS·CH_3CN is blocked by the CH_3CN guests with no color change under UV light irradiation. A low degree of structural isomerization was occurred in Cu_2I_2-TNDS-100 with a color change from yellow to yellow-green in the solid state when partly removing the CH_3CN guests. Besides, a high degree of structural isomerization was occurred in Cu_2I_2-TNDS-150 with a more obvious color change from yellow to

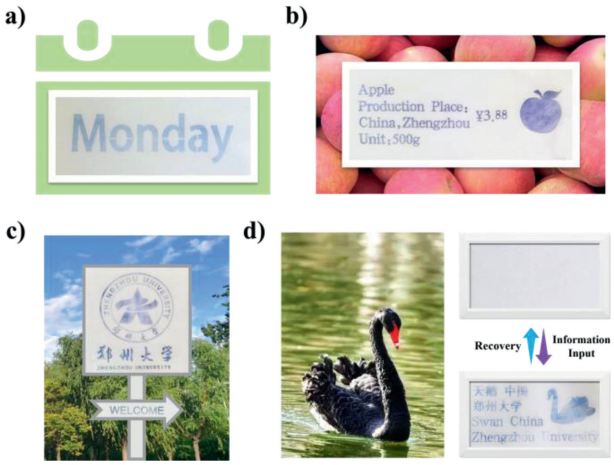

Fig. 5. The application of 150-coated film in short-term reusable-display: (a) Temporary calendar. (b) Short-term price-card for supermarket. (c) Billboards with information displays. (d) Short-term ID card images.

blue-green under the same external stimulus, when totally removing the CH_3CN guests. In addition, the blue-green color of Cu_2I_2-TNDS-150 can fade to yellow-green at a specific time (10 min) under heating at 80 °C. By taking advantage of the multiple and dynamic informational states in the Cu_2I_2-TNDS system, a dynamic 3D code and time-dependent information encryption were successfully achieved. The correct information can only be read under a specific condition. Furthermore, benefiting from the long retention time (>72 h) of MC form in Cu_2I_2-TNDS-150 under daylight conditions and good repeatability, short-term reusable materials such as temporary calendars, price-cards, billboards, and reusable identity cards were also prepared. This work demonstrates that multi-functional MOF-based smart materials can offer new opportunities for designing time-dependent information encryption and inkless erasable printing.

Declaration of competing interest

The authors declare that they have no known competing financial interests or personal relationships that could have appeared to influence the work reported in this paper.

Acknowledgments

This work was supported by the National Natural Science Foundation of China (Nos. 21825106, 92061201, 22105175), and Postdoctoral Research Grant in Henan Province (No. 202102001).

Supplementary materials

Supplementary material associated with this article can be found, in the online version, at doi:10.1016/j.cclet.2023.108491.

References

[1] K. Muller, J. Helfferich, F. Zhao, et al., Adv. Mater. 30 (2018) 1706551.
[2] S. Qin, H. Zou, Y. Hai, et al., Chin. Chem. Lett. 33 (2022) 3267–3271.
[3] Y. Sun, X. Le, S. Zhou, et al., Adv. Mater. 34 (2022) 2201262.
[4] F.D. J.ochum, P. Theato, Chem. Soc. Rev. 42 (2013) 7468–7483.
[5] Q. Wang, Z. Qi, M. Chen, et al., Aggregate 2 (2021) e110.
[6] Y. Xue, Z. Zhang, P. Shi, et al., Chin. Chem. Lett. 32 (2021) 539–542.
[7] Y. Li, Y.Y. An, J.Z. Fan, et al., Angew. Chem. Int. Ed. 59 (2020) 10073–10080.
[8] Y. Jiao, R.Q. Y.ang, Y.C. L.uo, et al., CCS Chem. 4 (2022) 132–140.
[9] Z. Wei, K. Zhang, C.K. K.im, et al., Chin. Chem. Lett. 32 (2021) 493–496.
[10] W. Lu, M. Si, X. Le, et al., Acc. Chem. Res. 55 (2022) 2291–2303.
[11] Z.G. Z.heng, H.L. H.u, Z.P. Z.hang, et al., Nat. Photo. 16 (2022) 226–234.
[12] Q. Xu, Z. Qin, Y. Bei, et al., Chin. Chem. Lett. 33 (2022) 4838–4841.
[13] Y. Jiang, C. Hu, H. Cheng, et al., ACS Nano 10 (2016) 4735–4741.

[14] C.X. M.a, X.X. L.e, X.L. T.ang, et al., Adv. Funct. Mater. 26 (2016) 8670–8676.
[15] Z.E. Zhang, Y.Y. An, B. Zheng, et al., Sci. China Chem. 64 (2021) 1177–1183.
[16] R. Piotrowska, T. Hesketh, H. Wang, et al., Nat. Mater. 20 (2021) 403–409.
[17] B. Garai, A. Mallick, R. Banerjee, Chem. Sci. 7 (2016) 2195–2200.
[18] D. Yan, Z. Wang, Z. Zhang, Acc. Chem. Res. 55 (2022) 1047–1058.
[19] X.Y. Ren, L.H. Lu, Chin. Chem. Lett. 26 (2015) 1439–1445.
[20] L.Z. Cai, Z.Z. Yao, S.J. Lin, et al., Angew. Chem. Int. Ed. 60 (2021) 18223.
[21] R.W. O.u, H.C. Z.hang, C. Zhao, et al., Chem. Mater. 32 (2020) 10621–10627.
[22] Z. Li, G. Wang, Y. Ye, et al., Angew. Chem. Int. Ed. 58 (2019) 18025–18031.
[23] D.E. W.illiams, C.R. M.artin, E.A. D.olgopolova, et al., J. Am. Chem. Soc. 140 (2018) 7611–7622.
[24] A.M. R.ice, C.R. M.artin, V.A. G.alitskiy, et al., Chem. Rev. 120 (2020) 8790–8813.
[25] H. Wang, X. Wang, R.M. Kong, et al., Chin. Chem. Lett. 32 (2021) 198–202.
[26] E.A. D.olgopolova, V.A. G.alitskiy, C.R. M.artin, et al., J. Am. Chem. Soc. 141 (2019) 5350–5358.
[27] X. Guo, T. Mao, Z. Wang, et al., ACS Cent. Sci. 6 (2020) 787–794.
[28] J. Park, D. Feng, S. Yuan, et al., Angew. Chem. Int. Ed. 54 (2015) 430–435.
[29] H. Zhou, W. Cao, N. Sun, et al., Chin. Chem. Lett. 32 (2021) 3123–3127.
[30] Y.X. Li, W. Zhong, J.J. Zhou, et al., Angew. Chem. Int. Ed. 61 (2022) e202212732.
[31] X. Meng, B. Gui, D. Yuan, et al., Sci. Adv. 2 (2016) e1600480.
[32] N. Yanai, T. Uemura, M. Inoue, et al., J. Am. Chem. Soc. 134 (2012) 4501–4504.
[33] S. Krause, J.D. E.vans, V. Bon, et al., Nat. Commun. 13 (2022) 1951.
[34] B. Yuan, G. Gou, T. Fan, et al., Angew. Chem. Int. Ed. 61 (2022) e202204568.
[35] H. Zhou, J.J. H.an, J. Cuan, et al., Chem. Eng. J. 431 (2022) 134170.
[36] D. Li, Z. Feng, Y. Han, et al., Adv. Sci. 9 (2022) 2104790.
[37] X.Ren Yang, L. Mei, et al., Angew. Chem. Int. Ed. 61 (2022) e202117158.
[38] Q. Wang, B. Lin, M. Chen, et al., Nat. Commun. 13 (2022) 4185.
[39] H. Ju, C.N. Z.hu, H. Wang, et al., Adv. Mater. 34 (2022) 2108163.
[40] J. Tan, Q. Li, S. Meng, et al., Adv. Mater. 33 (2021) 2006781.
[41] X.Z. S.ong, S.Y. S.ong, S.N. Z.hao, et al., Adv. Funct. Mater. 24 (2014) 4034–4041.
[42] S. Garg, H. Schwartz, M. Kozlowska, et al., Angew. Chem. Int. Ed. 58 (2019) 1193–1197.
[43] Y. Yang, Q. Li, H. Zhang, et al., Adv. Mater. 33 (2021) 2105418.
[44] H. Xie, Z. Li, J. Gong, et al., Adv. Mater. 33 (2021) 2105113.